

See discussions, stats, and author profiles for this publication at: <https://www.researchgate.net/publication/345008026>

How Were the Eastward-Moving Heavy Rainfall Events from the Tibetan Plateau to the Lower Reaches of the Yangtze River Enhanced?

Article in *Journal of Climate* · October 2020

DOI: 10.1175/JCLI-D-20-0226.1

CITATIONS

3

READS

322

8 authors, including:



Yang Zhao

Chinese Academy of Meteorological Sciences

32 PUBLICATIONS 264 CITATIONS

[SEE PROFILE](#)



Deliang Chen

University of Gothenburg

507 PUBLICATIONS 17,210 CITATIONS

[SEE PROFILE](#)



Yi Deng

Georgia Institute of Technology

125 PUBLICATIONS 1,845 CITATIONS

[SEE PROFILE](#)



S.-W. Son

Seoul National University

132 PUBLICATIONS 4,410 CITATIONS

[SEE PROFILE](#)

Some of the authors of this publication are also working on these related projects:



Dynamics and importance of convection in the Tibetan Plateau region [View project](#)



Impact of climate change on water balance on The Third Pole Region [View project](#)

How Were the Eastward-Moving Heavy Rainfall Events from the Tibetan Plateau to the Lower Reaches of the Yangtze River Enhanced?

YANG ZHAO,^{a,b} DELIANG CHEN,^c YI DENG,^d SEOK-WOO SON,^b XIANG WANG,^e DI DI,^f MENGTING PAN,^e
AND XIAODAN MA^f

^a State Key Laboratory of Severe Weather, Chinese Academy of Meteorological Sciences, Beijing, China

^b School of Earth and Environmental Sciences, Seoul National University, Seoul, South Korea

^c Regional Climate Group, Department of Earth Sciences, University of Gothenburg, Gothenburg, Sweden

^d School of Earth and Atmospheric Sciences, Georgia Institute of Technology, Atlanta, Georgia

^e Institute for Climate and Application Research, Nanjing University of Information Science and Technology, Nanjing, China

^f Key Laboratory for Aerosol–Cloud–Rain of China Meteorological Administration, School of Atmospheric Physics, Nanjing University of Information Science and Technology, Nanjing, China

(Manuscript received 1 April 2020, in final form 29 August 2020)

ABSTRACT: This study investigates eastward-moving summer heavy rainfall events in the lower reaches of the Yangtze River (LRYR), which are associated with the Tibetan Plateau (TP) vortices. On the basis of rainfall data from gauges and additional atmospheric data from ERA-Interim, the dynamic and thermodynamic effects of moisture transport and diabatic heating are estimated to determine the physical mechanisms that support the eastward-moving heavy rainfall events. As the rainband moves eastward, it is accompanied by anomalous cyclonic circulation in the upper and middle troposphere and enhanced vertical motion throughout the troposphere. In particular, the rainfall region is located in the fore of the upper-level trough, which is ideal for baroclinic organization of the convective system and further development of the eastward-moving vortex. The large atmospheric apparent heat source (Q_1) also contributes for lifting the lower-level air into the upper atmosphere and for enhancing the low-level convective motion and convergence during the heavy rainfall process. Piecewise potential vorticity inversion further verifies the crucial role that the diabatic heating played in developing the anomalous geopotential height favorable for the enhanced rainfall. The combined action of the dynamic and thermodynamic processes, as well as the rich moisture supply from the seas, synergistically sustained and enhanced the eastward-moving rainfall.

KEYWORDS: Atmospheric circulation; Cyclogenesis/cyclolysis; Extratropical cyclones; Hydrologic cycle

1. Introduction

Heavy rainfall is one of the most common natural hazards in the world. It usually has a cause-and-effect relationship with flooding, landslides, debris flows, and urban inland inundation. It can lead to huge economic losses and casualties (Salinger and Griffiths 2001; Downton and Pielke 2005; Kundzewicz et al. 2014; Wang et al. 2015). East Asia is not an exception. For instance, China is prone to floods, frequently with huge economic consequences and negative social impacts (Wu et al. 2006; Zhang and Zhou 2015). In particular, the Yangtze River Basin (YRB) experiences heavy rainfall nearly every summer. Many cities in the YRB are major economic and industrial centers (Zong and Chen 2000). Therefore, improving the comprehension of flood hazards in the YRB is of importance to society in general and to the research community in particular.

While the importance of heavy rainfall over the YRB is widely acknowledged, our understanding of heavy rainfall events over the YRB and their physical mechanisms remains limited. Many previous studies have explored the influence of large-scale circulation on heavy rainfall events in the YRB. Xiao et al. (2014) reported that summer heavy rainfall over the

YRB is influenced by both El Niño–Southern Oscillation (ENSO) and the Indian Ocean dipole (IOD). They particularly indicated that a negative ENSO a year earlier tends to increase the frequency of intensive rainfall in the lower reaches of the Yangtze River (LRYR). Other studies have suggested that the frequency of heavy rainfall events over the YRB is negatively correlated with the intensity of the East Asian summer monsoon, and the mei-yu front plays a key role in this negative correlation (Zhang et al. 2008; Wang and Yang 2017).

Huang and Qian (2004) suggested that an intensified South Asian high tends to trigger flooding in the middle and lower reaches of the YRB. Hu et al. (2018) later confirmed that heavy rainfall over the middle reach of the Yangtze River has a close relationship with anomalous moisture convergence, which is triggered by the eastward expansion of the South Asian high and intensification of the westerly jet. Chen and Zhai (2016) documented that not only the South Asian high but also the western Pacific subtropical high (WPSH) are important for the persistent heavy rainfall events over the YRB.

Shi et al. (2008) emphasized that the Tibetan Plateau (TP) topography plays a substantial role in generating and reinforcing the mesoscale disturbances, which in turn increase the sensible heat flux over the TP and propagate eastward to trigger the convection and rainfall in the YRB. The TP can block the summer monsoon, creating moisture convergence at

Corresponding author: Deliang Chen, deliang@gvc.gu.se

DOI: 10.1175/JCLI-D-20-0226.1

© 2020 American Meteorological Society. For information regarding reuse of this content and general copyright information, consult the [AMS Copyright Policy](#) (www.ametsoc.org/PUBSReuseLicenses).

the eastern fringe of the TP and promoting moisture transport to the LRYR (Xu et al. 2008). In this way, the rainfall over the LRYR is affected by the upstream TP.

The TP is sometimes referred to as the third pole, and it deeply affects the weather and climate of the Asian continent (Hsu 2003; Hunt et al. 2018; Qian et al. 2011; Duan et al. 2012; Yang et al. 2014). Ge et al. (2019) suggested that the TP heating could affect the South Asian high, although the relationship between the TP heating and summer heavy rainfall in eastern China is still unclear. The stronger the heating, the greater the eastern extension of the South Asian high (Zhang et al. 2002; Duan et al. 2012), which can enhance the moisture transport to eastern China. In summer, the heating over the TP is larger than other places at similar latitudes (Duan and Wu 2005; Duan and Xiao 2015). Consequently, the thermal conditions over the TP could influence the summer monsoon activity and then affect the location and intensity of rainfall in the LRYR. Moreover, convective systems occur frequently over the TP during summer (Qie et al. 2014; Li and Zhang 2017; Kukulies et al. 2019), and some of these convective systems could move off the TP to the downstream (Curio et al. 2019).

Zhao et al. (2018, 2019a) also showed that mesoscale to synoptic-scale vortices initiated over the TP and could also move off the TP. It helps to bring moisture from the Southern Ocean (see also Li et al. 2017). They could result in heavy rainfall events over the LRYR. It was also pointed out using water vapor transport analysis that the migrating vorticity structure out of the TP can be enhanced and kept moving eastward. When the vorticity structure travels over the LRYR, heavy rainfall can be generated. Therefore, the convective system over the TP can be regarded as a precursor for heavy rainfall over the LRYR. Zhao et al. (2016a) determined that cloud over the LRYR could be tracked back to the TP. They showed the correlative relationship between rainfall over the LRYR and a banded low-cloud structure from the TP to the LRYR along the Yangtze River. These results indicate that the TP vortex and the associated convective system can be regarded as a precursor for heavy rainfall over the LRYR.

Despite the existing large body of literature on heavy rainfall over the YRB, a systematic characterization of the dynamic and thermodynamic backgrounds associated with eastward-moving rainfall events along the Yangtze River is still rare, especially with regard to the physical mechanisms associated with the rainfall evolution toward its strengthening. This study addresses this knowledge gap by focusing on the thermal and dynamic features during the entire eastward-moving rainfall process, which ends up with heavy rainfalls in the LRYR. The present study addresses this knowledge gap by focusing on the thermal and dynamic features during the entire life cycle of eastward-moving rainfall events, which end up with heavy rainfall in the LRYR.

2. Data and methods

a. Data

To identify the eastward-moving rainfall event, a rainfall dataset including more than 2400 daily rainfall gauge stations

from 1980 to 2016 is used. These data, released by the National Meteorological Information Center (NMIC) of the China Meteorological Administration (<http://data.cma.cn/>), cover nearly the whole of the China mainland (Zhong et al. 2016; Zhao et al. 2018, 2019b). To address the dynamic and thermodynamic characteristics of eastward-moving rainfall events, 6-hourly atmospheric fields for 1980 to 2016 were acquired from ERA-Interim (<http://apps.ecmwf.int/datasets/>) produced by the European Centre for Medium-Range Weather Forecasts (ECMWF) (Dee and Uppala 2009; Dee et al. 2011). This dataset has improved humidity analysis and has assimilated the satellite passive microwave data for the total column moisture in areas affected by cloud and rain, compared with the previous reanalysis from the ECMWF. The $0.75^\circ \times 0.75^\circ$ horizontal resolution data were used in this study. The variables of horizontal winds, vertical motion, specific humidity, temperature, and geopotential height were used. To ensure consistency with the time of the observational data from the rainfall gauges, the analysis data were converted to the local time [Beijing time (BJT)] in this study.

b. Methods

1) EASTWARD-MOVING RAINFALL EVENTS

Previous studies have defined the heavy rainfall level as the rainfall that exceeds 50 mm in 24 h (Zhao et al. 2016b; Liu et al. 2016; Xu et al. 2017). We choose the eastward-moving rainfall events originating from the TP, which cause heavy rainfall (equal to or greater than 50 mm day^{-1}) for at least 31 gauges in the LRYR. Zhao et al. (2016b) investigated the moisture transport channels for the heavy rainfall in east China mainly converging in the lower reaches of the Yangtze River. Moreover, the heavy rainfall in the LRYR has a strong correlational relationship with the cloud that derived from the TP and transport to the LRYR along the Yangtze River (Zhao et al. 2016a). Hence, the LRYR is defined as $27^\circ\text{--}33^\circ\text{N}$, $110^\circ\text{--}122.5^\circ\text{E}$ in this study and a total of 311 observational gauges are included in the LRYR. Such a rectangular box makes the diagnostics much easier and straightforward, as the meteorological data were on regular grids. The eastward-moving rainfall events are selected from 1980 to 2016.

The number of heavy rainfall events, which cover at least 31 gauges (10%) in the LRYR region, is 205 during the summers from 1980 to 2016. Among them, 51 events are identified as eastward-moving heavy rainfall events by analyzing the rainfall distribution and tracing the rainfall-related vorticity at 500, 700, and 850 hPa (Fig. 1). Nearly all of them take 3 to 5 days to travel from the TP to the LRYR. To facilitate composite analysis, the heavy rainfall events whose lifetime is 4 days are selected. This allows a total of 27 events (Table 1). The 4-day events account for 53% of all eastward-moving heavy rainfall events, effectively representing the main features of the eastward-moving heavy rainfall events. Although not shown, the overall results do not change much when all 51 events are examined. Composite analysis is used to study the common features of the evolution of the eastward-moving heavy rainfall events and the associated dynamic and thermodynamic processes.

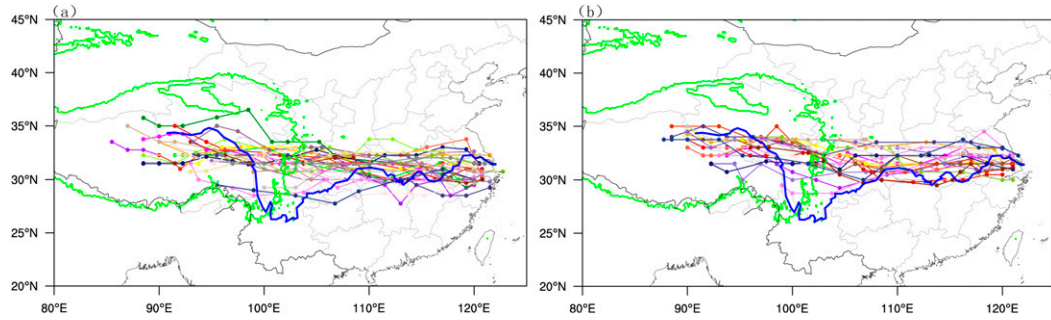


FIG. 1. The eastward-moving vorticities originating from the TP based on 6-hourly ERA-interim data for 1980–2016. The rainfall intensity in the LRYR region is (a) 50–100 mm day⁻¹ and (b) ≥100 mm day⁻¹. The different colored lines represent the trajectory of different heavy rainfall events. The green line marks the terrain elevation of 3000 m and the blue line shows the Yangtze River. The dots are the centers of the vorticities.

2) ATMOSPHERIC APPARENT HEAT SOURCE

The atmospheric apparent heat source (Q_1) is calculated based on the thermodynamic equation. The Q_1 has been widely applied to study the thermodynamic effect over the TP (Zhao and Chen 2001; Xu et al. 2013; Wang et al. 2019). However, the use of Q_1 to study eastward-moving heavy rainfall is rare. The equation is as follows:

$$Q_1 = C_p \left[\frac{\partial T}{\partial t} + \mathbf{V} \cdot \nabla T + \omega \left(\frac{P}{P_0} \right)^k \frac{\partial \theta}{\partial P} \right], \quad (1)$$

where \mathbf{V} and ω are the horizontal wind fields and vertical motion in pressure coordinates, respectively, T denotes the atmosphere temperature, P_0 is the surface pressure and set to be 1000 hPa here, θ is the potential temperature, C_p represents the specific heat, and the constant k is equal to 0.286. The vertically integrated Q_1 is written as

$$\langle Q_1 \rangle = LP + S + \langle Q_R \rangle, \quad (2)$$

where L is the latent heat of condensation, P is the rainfall amount, S is the surface sensible heat flux, and $\langle Q_R \rangle$ is the radiative heating. For the vertical integration of Q_1 , the top

level is set at 100 hPa and the bottom is set to the level that is closest to and higher than the surface in different grids.

3) POTENTIAL VORTICITY INVERSIONS

Potential vorticity (PV) has two important features: one is the conservation in the adiabatic heating process and the other is the evolution affected by the diabatic heating. On the basis of these two characteristics, Hoskins et al. (1985) explained the PV anomaly corresponding to the features and development of weather systems in the upper and lower levels based on the quasigeostrophic (QG) equilibrium. PV analysis is applied to study the large-scale atmospheric feature. The spatial scale of the anomalous eastward-moving vortex belongs to the synoptic scale. As such, the QG PV q is defined as

$$q = \frac{1}{f_0} \nabla^2 \phi + f + \frac{\partial}{\partial p} \left(\frac{f_0 \partial \phi}{\sigma \partial p} \right), \quad (3)$$

where f is the Coriolis parameter (s^{-1}) and f_0 is the reference f , which is set to $10^{-4} s^{-1}$ for the synoptic scale in the midlatitude, ϕ is the geopotential height (m), and $\sigma = \sigma(p)$ is the static stability parameter ($m^4 s^2 kg^{-2}$). The first term on the right side of Eq. (3) is the geostrophic relative vorticity, the second term

TABLE 1. The start and end dates of the selected 27 eastward-moving heavy rainfall events that last for 4 days.

Event No.	Start and end dates	Event No.	Start and end dates
1	4 Jun–7 Jun 1980	15	9 Jun–12 Jun 1998
2	6 Jul–9 Jul 1980	16	19 Jul–22 Jul 1998
3	14 Jul–17 Jul 1980	17	27 Aug–30 Aug 1999
4	9 Aug–12 Aug 1980	18	16 Aug–19 Aug 2000
5	17 Jun–20 Jun 1983	19	7 Jun–10 Jun 2001
6	19 Jun–22 Jun 1986	20	12 Jun–15 Jun 2004
7	18 Aug–21 Aug 1987	21	6 Jun–9 Jun 2008
8	16 Jun–19 Jun 1988	22	6 Jun–9 Jun 2009
9	24 Jun–27 Jun 1989	23	6 Jun–9 Jun 2010
10	29 Jun–2 Jul 1990	24	15 Jun–18 Jun 2011
11	27 Jun–30 Jun 1991	25	11 Jul–14 Jul 2012
12	1 Aug–4 Aug 1991	26	4 Jun–7 Jun 2013
13	11 Jun–14 Jun 1992	27	23 Jun–26 Jun 2014
14	12 Jun–15 Jun 1995		

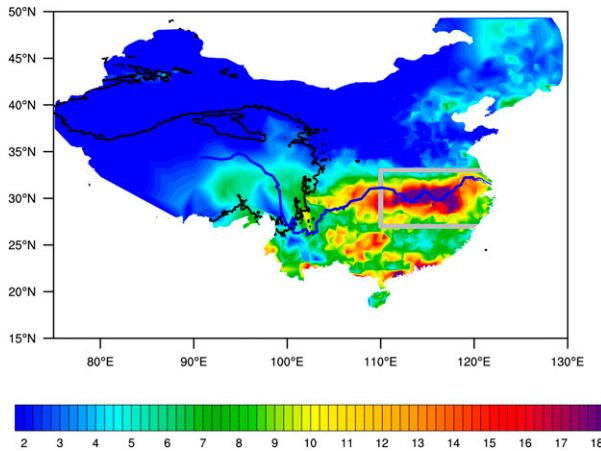


FIG. 2. The daily average rainfall (colors; unit: mm day^{-1}) from day 1 to 4 of the 27 selected heavy rainfall events. Blue solid line is the Yangtze River, and the black solid line is the 3000-m height, representing the main body of the TP. The LRYR is denoted in gray.

represents the planetary vorticity, and last term stands for the stretching vorticity.

We want to obtain the generation of PV from the diabatic heating processes in the QG framework (Lu and Deng 2015). Based on a study by Black and Dole (1993), the relationship between the anomalous PV (q' ; unit: s^{-1}) and the corresponding anomalous geopotential height; (ϕ' ; unit: m) can be described as

$$q' = \frac{1}{f_0} \nabla^2 \phi' + f_0 \frac{\partial}{\partial p} \left(\frac{1}{\sigma} \frac{\partial \phi'}{\partial p} \right), \quad (4)$$

where $q' = q - q_{\text{ref}}$ and the reference field q_{ref} is expressed as a 30-day temporal average (Teubler and Riemer 2016). The selected 4-day heavy rainfall events are included in this time period. The anomalous geopotential height ϕ' is computed by inverting Eq. (4). The equation implies that the PV anomaly induced by the diabatic heating can be translated into the corresponding response of the geopotential height anomaly. It can be used to predict how PV anomalies affect the evolution of large-scale flow.

4) WHOLE-LAYER WATER VAPOR FLUX

The whole-column moisture flux was calculated to quantify the contribution of anomalous moisture to the rainfall region as follows:

$$qu(x, y, t) = \frac{1}{g} \int_{100\text{hPa}}^{1000\text{hPa}} q(x, y, p, t) u(x, y, p, t) dp, \quad (5)$$

$$qv(x, y, t) = \frac{1}{g} \int_{100\text{hPa}}^{1000\text{hPa}} q(x, y, p, t) v(x, y, p, t) dp, \quad (6)$$

where qu and qv are the zonal and meridional moisture flux, q is the specific humidity, u and v are the zonal and meridional wind fields, and g is the gravity.

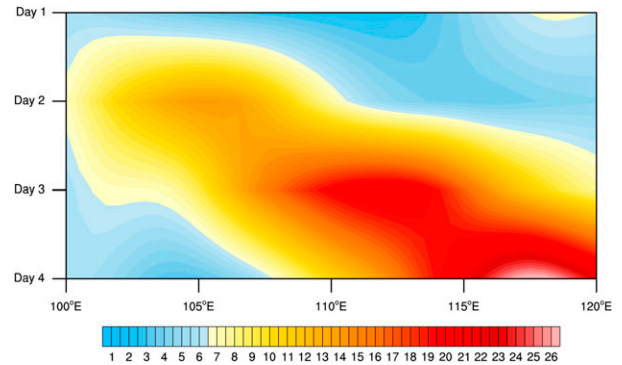


FIG. 3. Hovmöller diagram of the daily average rainfall of the 27 heavy rainfall events, averaged over the latitude band 27.5° – 33° N. The shaded contour shows the rainfall intensity (unit: mm day^{-1}).

3. Results

a. Features of the composite heavy rainfall process

Figure 2 shows the composite daily mean rainfall during the 27 selected heavy rainfall events that lasted 4 days, displaying a clear east–west distribution along the Yangtze River. The rainfall in the LRYR clearly shows a band structure. Interestingly, the westernmost location of the rainband is found in the central and eastern TP. In addition, the rainfall gradually increases from west to east along the YRB as shown in Fig. 2, which demonstrates the enhancement of the rainfall systems during their movements from the TP to the LRYR.

Zhang and Tao (2002) found that the persistent heavy rainfall in the YRB in the summer of 1998 was triggered by eastward-moving TP vortexes. They used the blackbody temperature (TBB) data with the time–longitude profile and found the BBT structure is eastward moving. They assumed that the moving convective system was coupled with the BBT. To illustrate the feature of the eastward-moving rainfall, the composite time–longitude cross section of the 27 heavy rainfall events along the LRYR latitude range (27° – 33° N) is calculated. The rainfall contour clearly shows an eastward-moving structure (Fig. 3). It also clearly shows an increasing intensity of rainfall moving from west to east with time. The rainfall is substantially enhanced around 110° E, which is the western boundary of the LRYR.

To further highlight the synthesis features of the eastward-moving rainfall events, we divided the region of the eastward-moving rainfall events leading to heavy rainfall in the LRYR into four sections (areas A, B, C, and D in Fig. 4a) based on the location of the rainfall center (Figs. 4b–e). On day 1, the rainfall was generated over the central and eastern TP (Fig. 4b). On day 2, the rainfall left the TP and moved eastward with itself being strengthened (Fig. 4c). On day 3, the rain kept moving eastward to the middle reaches of the Yangtze River and was further enriched (Fig. 4d). On day 4, the rainfall center reached the LRYR, and the intensity of the rainfall increased to the heavy rainfall level (Fig. 4e). By taking account of the above rainfall features, we verify that the rainfall originated from the TP was transported eastward. As a result, heavy rainfall occurs in the LRYR.

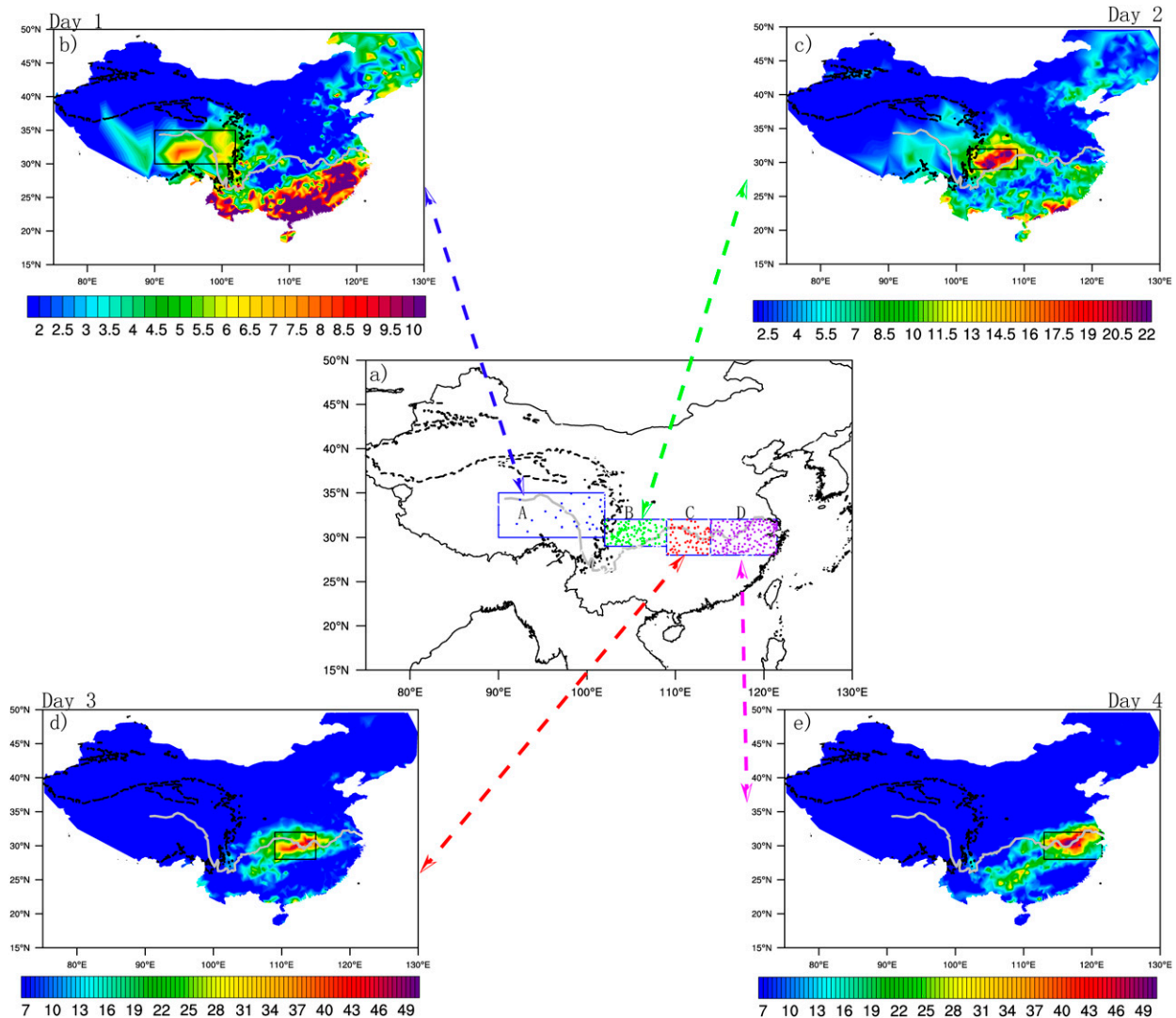


FIG. 4. Daily mean rainfall amount for each of the 4 days of the 27 heavy rainfall events (contour; unit: mm day^{-1}). (a) Boxes A (30° – 35°N , 90° – 102°E), B (29° – 32°N , 102° – 109°E), C (28° – 32°N , 109° – 114°E), and D (28° – 32°N , 114° – 121.5°E) correspond to the main rainfall regions, illustrating the daily mean rainfall amount of days (b) 1, (c) 2, (d) 3, and (e) 4, respectively. The colored dots in (a) are the observational rainfall stations in different regions, and the gray solid line indicates the Yangtze River. The black dashed line means an elevation of 3000 m, which represents the main body of the TP.

b. The dynamics of the eastward-moving rainfall process

So far, the eastward-moving features of the rainfall have been determined, but a question remaining to be answered is how the rainfall is enhanced and what role the anomalous horizontal and vertical atmospheric motions play. To answer these questions, we explore the anomalous vorticity structure propagating from the central and eastern TP to the east of the YRB. Combined with Figs. 4 and 5, the anomalous cyclone or vertical motion and the rainfall are closely coupled with each other. We find that the anomalous system reaches to the LRYR and was derived from the TP (Fig. 5). At the initial phase, as shown in Fig. 5a, the vorticity system originated from the central and eastern TP at 500 hPa (the surface ground

average height of the TP is close to 4000 m). The vorticity is much stronger than that in the surrounding area on day 1. On day 2, the vorticity had moved off the TP and was located in the Sichuan Basin, to the east of the TP. The southwest airflow from the Bay of Bengal (BOB) and South China Sea (SCS) transports moisture to the vorticity system (Fig. 5b; green circle). On day 3, the anomalous vorticity system reached the western part of the LRYR. Compared with the previous phases, the intensity of anomalous vorticity was substantially reinforced and enlarged (Fig. 5c; green circle). On day 4, the anomalous vorticity system controlled the whole LRYR region and its intensity continued to be reinforced (Fig. 5d; green circle). Notably, there was sufficient moisture transported to the YRB at the front of the anomalous vorticity (Figs. 4b–d).

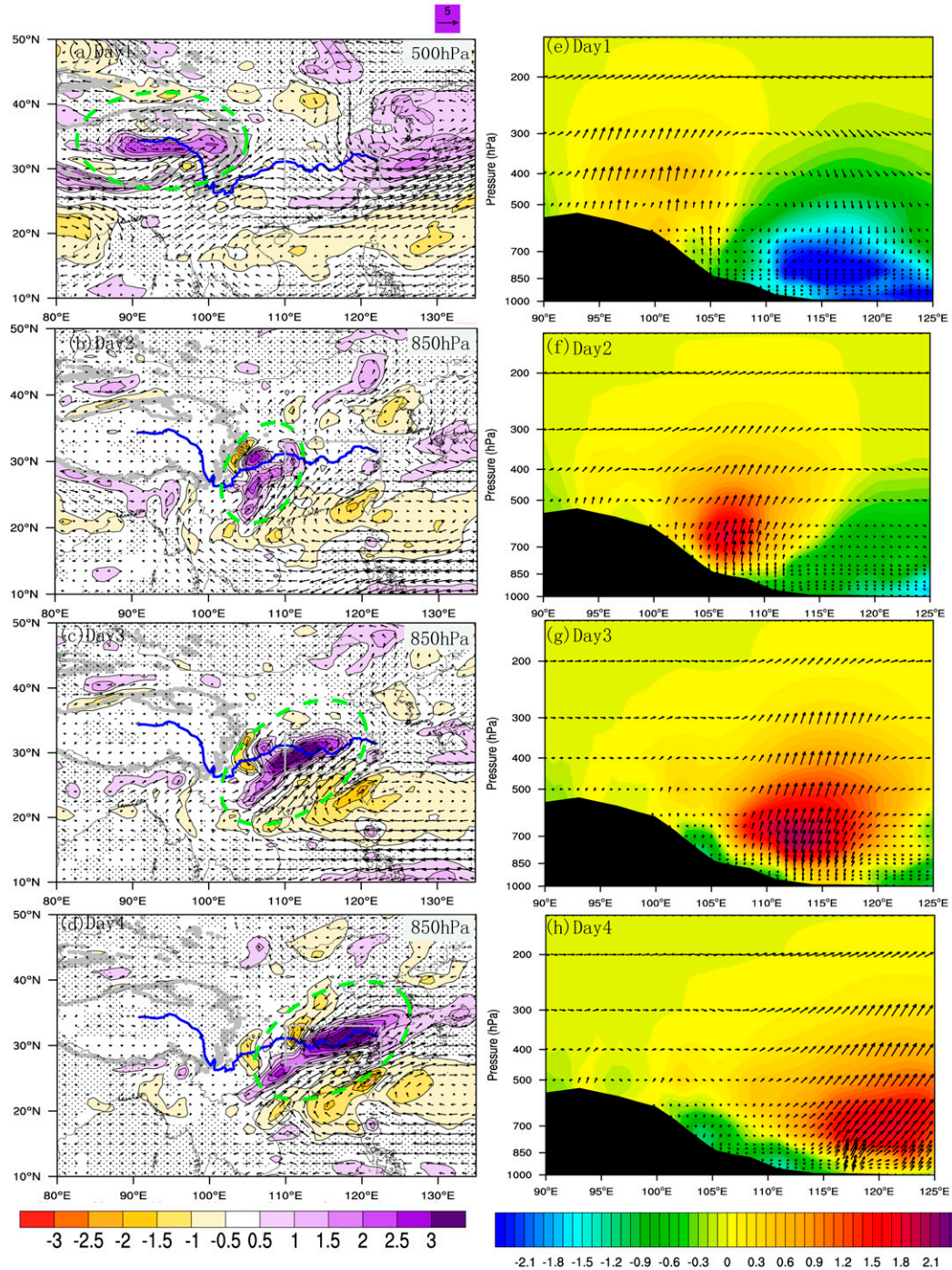


FIG. 5. Anomalous wind fields (arrows; unit: m s^{-1}) and vorticity field (contours; 10^{-5} s^{-1}) that are statistically significant above the 90% confidence level at (a) 500 and (b)–(d) 850 hPa between the daily mean of the 27 four-day heavy rainfall process events and the climate daily mean. Gray box represents the LRYR. The gray line is the part of the TP and the blue line presents the Yangtze River. (e)–(h) Anomalous cross sections of vertical motion (unit: m s^{-1}) along the latitude center of vorticity. The times respectively correspond to (a)–(d). The contours in (e)–(h) represent the specific humidity levels (unit: g kg^{-1}). The black colored area is part of the TP.

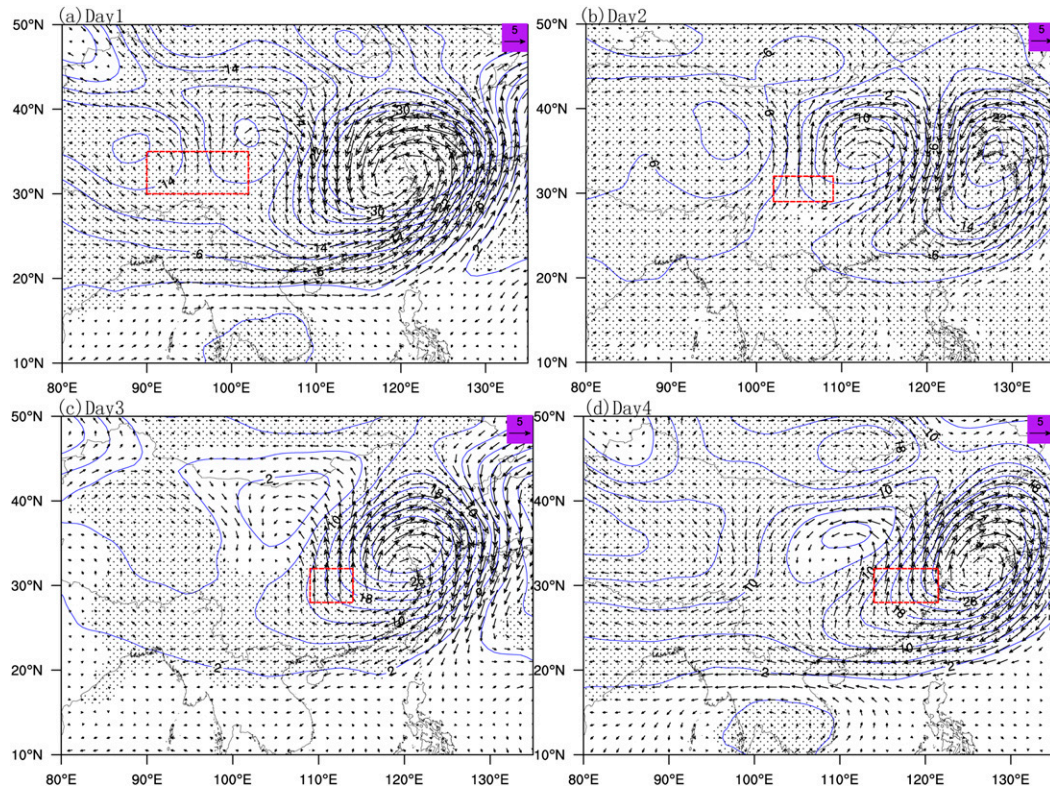


FIG. 6. Difference wind (arrows; unit: m s^{-1}) and geopotential height fields (blue line; m) at 200 hPa between the daily map and average map of heavy rainfall events. Red dashed boxes are the key rainfall region on each day, as shown in Fig. 4. Dots indicate composite anomalies of geopotential height exceeding the 90% confidence level.

The results show that the anomalous cyclone structure in the heavy rainfall process kept moving eastward until it reached the LRYR, and the intensity of the cyclonic system was continuously reinforced.

The anomalous vertical motion can also be found over the TP on day 1, especially at the eastern part of the TP (Fig. 5e). On day 2, the vertical structure had reached the eastern edge of the TP, and the anomalous magnitude of specific humidity is obviously larger than on day 1 (Fig. 5f). On day 3, the vertical motion continued to move eastward and the moisture content kept increasing (Fig. 5g). On day 4, the vertical motion structure moved to the east of the YRB (Fig. 5h). In the entire rainfall eastward-moving process, the vertical motion starting from the surface could reach to 200 hPa as shown in Figs. 5e–h. The anomalous vertical motion system associated with the anomalous cyclone structure is favorable for the occurrence of the heavy rainfall.

Low-level synoptic systems can be steered by the upper-level flows. We thus examine the anomalous horizontal winds and geopotential field at 200 hPa. To highlight the anomalous vortex structure, the difference in wind fields and geopotential height field between the daily average of the composite heavy rainfall days and the daily average of composite heavy rainfall events on each of the 4 days [S_i ($i = 1, 2, 3, 4$) $- S_{\text{mean}}$, where S is the daily mean of composite heavy rain on days 1 to 4] are calculated. The results show that during the heavy rainfall events, the atmospheric circulation shows an anomalous

“dipole” form. This means that an anomalous cyclonic deviation and anticyclonic deviation exist around the rainfall region at 200 hPa. The intermediate region of the anomalous cyclonic circulation and anticyclonic circulation is over the rainfall region, where the geopotential height gradient gets larger (Fig. 6). The intermediate region of the so-called dipole is favorable for convective motion from below. Moreover, this dipole shows an eastward-moving state during the heavy rainfall process with time. On day 1, the dipole was located over the eastern of the TP (Fig. 6a). On day 2, the dipole moved off the TP and stayed over the middle part of mainland China (Fig. 6b). In the later days, the dipole structure continued to move eastward (Figs. 6c,d). Finally, the dipole system moved to eastern China, which is in harmony with the low-level system and vertical motion (Fig. 5).

At the middle level (500 hPa), the anomalous cyclonic structure obviously controls the rainfall region during the eastward moving process (Fig. 7). Moreover, the rainfall band is always located in the front of the trough. The anomalous cyclonic and trough structures are favorable for the vertical motion, enhancing the intensity of precipitation. The wind field is supposed to be in the quasigeostrophic state. The development of potential height is proportional to the absolute vorticity advection and differential thickness advection. At the middle level, there is a positive absolute vorticity advection in the front of the trough, lowering the potential height and

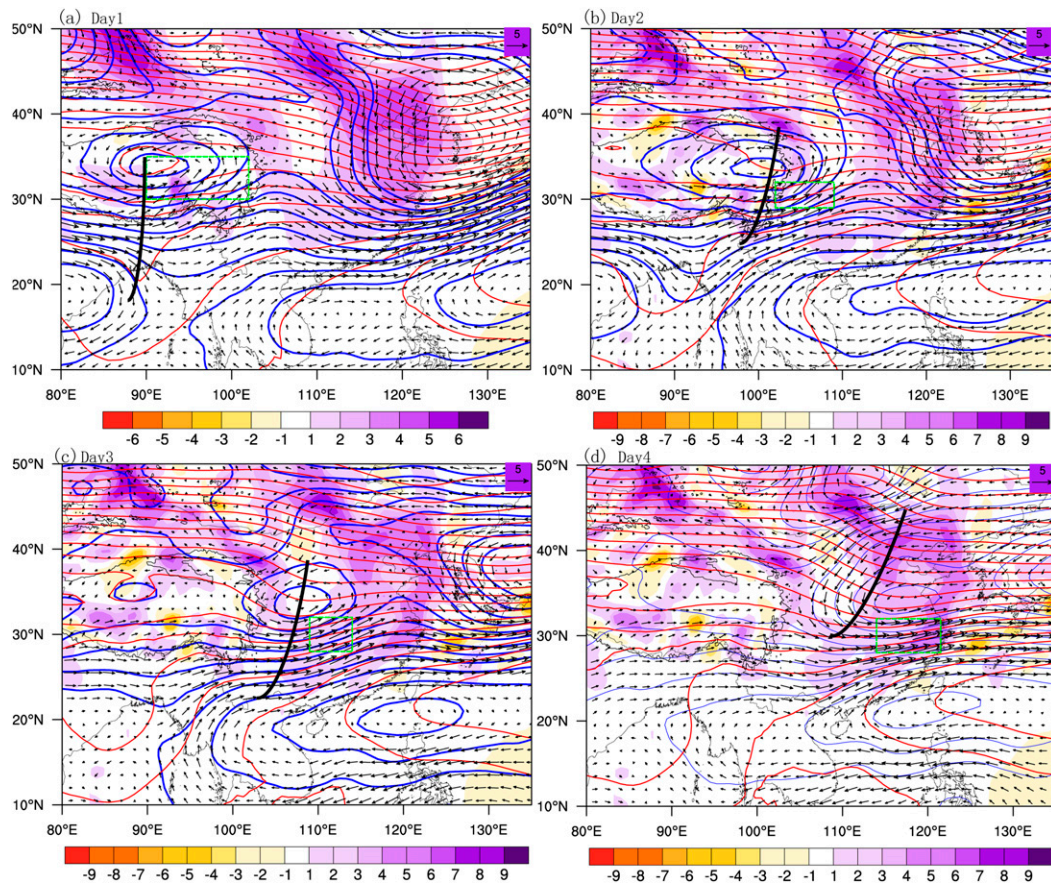


FIG. 7. Anomalous wind fields (arrows; unit: m s^{-1}) and geopotential height field (blue line; m) at 500 hPa between the daily mean of the 27 four-day heavy rainfall process events and the climate daily mean. The composite daily mean geopotential height (red line; unit: m) and the absolute vorticity advection (color shading; unit: 10^{-5} s^{-2}) for each of the 4 days of the 27 heavy rainfall events. The green box is the key region for each day, as shown in Fig. 4. The black line represents the trough. The gray curve line shows the terrain height at 3000 m and represents the TP.

pressure and helping the cyclonic structure develop and keep eastward moving (Fig. 7). At the initial phase, a warm advection maximizes between 200 and 400 hPa over the TP, which also helped decrease the surface low pressure and promote the development of surface vortex. The difference thickness advection is not obvious in other phases (figures not shown).

Compared with the circulation feature for all of the eastward-moving heavy rainfall days and other non-eastward-moving heavy rainfall days in the LRYR, all of the heavy rainfall events are characterized by the anomalous cyclone structure at the middle level, which controls the rain region. For the eastward-moving events, the anomalous cyclonic structure exhibits an east-west orientation. For other events, the anomalous cyclone has a northeast-southwest orientation. The wind field of the former (Fig. 8a) that comes from the south of TP is stronger than the latter (Fig. 8b). It illustrates that there is a circulation difference between the eastward-moving events and non-eastward-moving events at the middle level. The circulation of former favors the system transporting from the upstream.

In the selected eastward-moving rainfall process, the anomalous cyclone system and vertical motion correspond to the location

of the rainfall centers very well. Moreover, the anomalous structure in the upper-middle layer is favorable to maintain the eastward movement and the moisture is transported to the front of the anomalous vortex in the lower layer. Via the dynamic structure of the upper, middle, and lower levels, the interaction between different levels is favorable for convective activity. The eastward-moving systems could help to maintain and develop the eastward-moving of the low pressure structure. Therefore, it is worth further exploring the thermodynamic conditions that influence the vorticity during the entire heavy rainfall process. To further advance the knowledge of the physical mechanism for the eastward-moving rainfall, we take a close look at the thermodynamic features. We use Q_1 in the following section to explore the thermal conditions for eastward-moving rainfall.

c. The thermodynamics of the eastward-moving rainfall process

The composite anomalous whole-layer atmospheric apparent heat source ($\langle Q_1 \rangle$) is used to analyze the thermodynamic

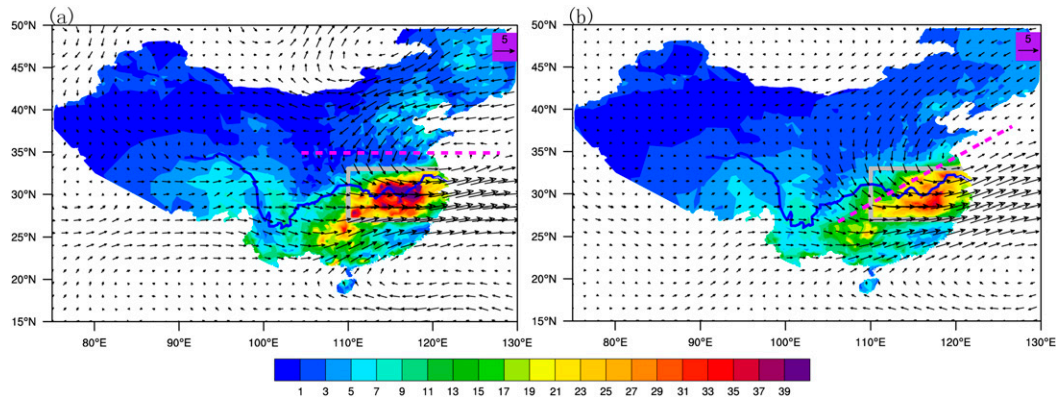


FIG. 8. (a) The anomalous wind fields (arrows; unit: m s^{-1}) at 500 hPa between the daily mean of all eastward-moving rainfall events (the last day of 51 events as shown in Fig. 1) and the climate daily mean. (b) As in (a), but for the other non-eastward-moving heavy rainfall events. The composite daily mean rainfall for heavy rainfall events (contours; unit: mm day^{-1}). The LRYR is in the gray solid box. The red dashed line represents the anomalous cyclone vortex trend.

environment. To highlight the thermodynamic features, the difference between $\langle Q_1 \rangle$ for the 27 heavy rainfall events for each of the 4 days and the climate daily mean are presented in Fig. 9. It is found that in the initial phase, the anomalous $\langle Q_1 \rangle$ has a large value over the central and eastern TP (Fig. 9a), and it corresponds to the location of the rainfall. On day 2, when the

rainfall center moved off the TP, the anomalously large value of $\langle Q_1 \rangle$ was still located over the rainfall area (Fig. 9b). On day 3, the larger region of anomalous $\langle Q_1 \rangle$ kept moving eastward, while the intensity of $\langle Q_1 \rangle$ was obviously strengthened (Fig. 9c). On day 4, the large-value area of anomalous $\langle Q_1 \rangle$ moved to the LRYR region and coexisted with the heavy rainfall (Fig. 9d).

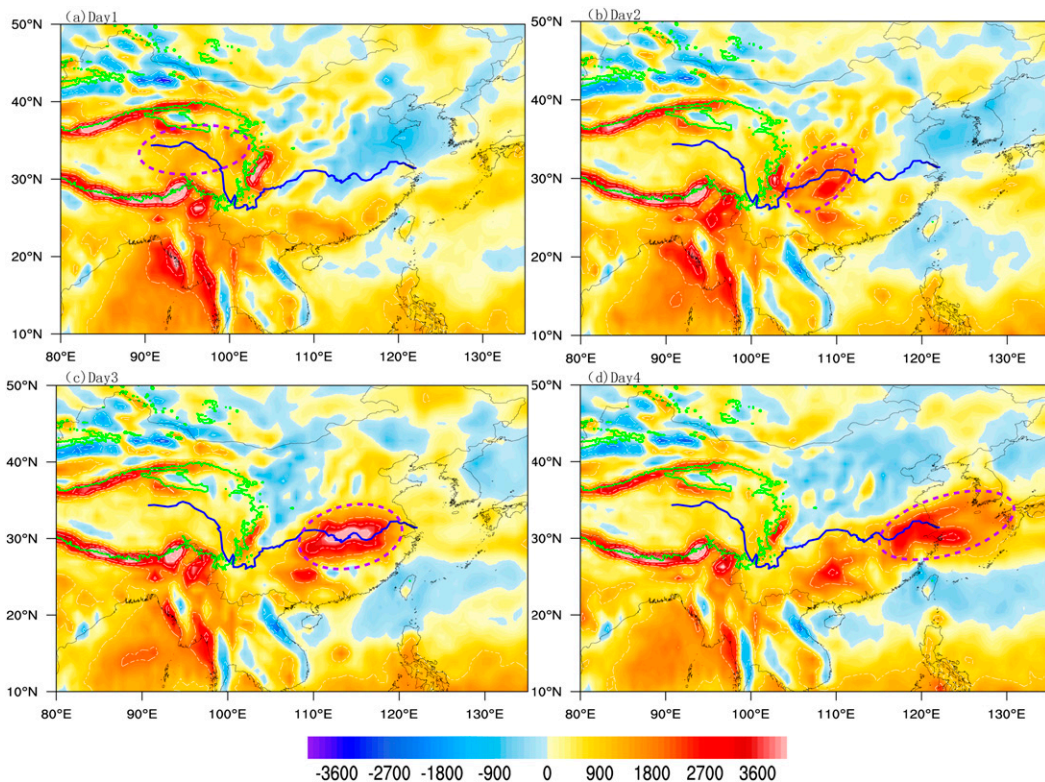


FIG. 9. Column-integrated apparent heat source anomaly $\langle Q_1 \rangle$ (contours; unit: W m^{-2}) on days (a) 1, (b) 2, (c) 3, and (d) 4 of the 27 heavy rainfall events. The purple dashed line denotes the approximate location of rainfall as shown in Fig. 4. The green line shows the terrain height at 3000 m and the blue line represents the Yangtze River.

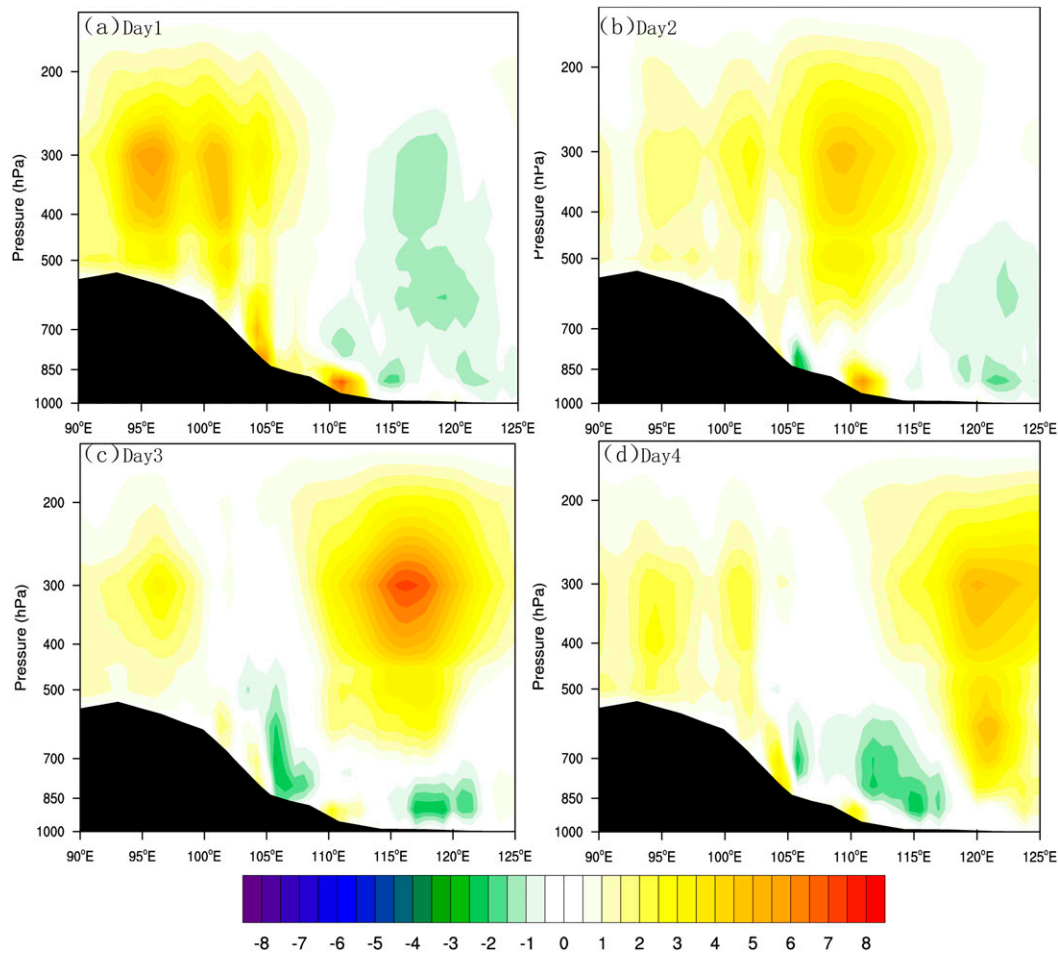


FIG. 10. Cross section of apparent heating rate anomaly q_1 (contour; unit: $\text{K s}^{-1} 10^{-4}$) on days (a) 1, (b) 2, (c) 3, and (d) 4 of the 27 heavy rainfall events. Black shading denotes part of the TP.

To show the evolution of Q_1 along the west–east direction, the pressure–longitude cross section along 33°N is shown in Fig. 10. We see that the single anomalous positive apparent heating rate derived from the eastern TP is moving to the LRYR region (Fig. 10). The largest-value center on all 4 days is located around the height of 300 hPa, whereas the relatively large apparent heating rate intensity is found from the middle and lower troposphere to the 200-hPa level. This means that almost the whole troposphere is heated during the heavy rainfall, which creates a large amount of latent heat. The effect of heating is helpful for the development of vertical motion. While the anomalous cyclone vortex brings moisture to the rainfall region and the convergence causes vertical motion, the associated condensation releases latent heat, which in turn adds more energy to feed convections, finally leading to the heavy rainfall over the LRYR.

d. PV inversion in response to the eastward-moving system

To further explore the evolution of the eastward-moving system associated with the diabatic heating effect, the quasi-geostrophic equilibrium PV is applied to investigate the role

played by the eastward-moving vortex for the heavy rainfall events. Piecewise PV inversion affords a rigorous method for supervising the circulation of a disturbance wave (based on the geopotential height) to diabatic heating changes (Winters and Martin 2017). The PV distribution shows great variation between different heavy rainfall events. To illustrate the importance of balanced flow anomalies, one eastward-moving heavy rainfall event is selected randomly (7–10 June 2001) as an example.

During the heavy rainfall process, the effect of diabatic heating is substantial. The changes in diabatic heating translate into changes in the PV generation (Lu and Deng 2015). In Fig. 11, the location of the rainfall is always in the trough or center of low pressure (blue lines). In the rainfall region, the geopotential height decreases (green solid lines) and it is favorable for the development of a trough. After the rainfall moves off the TP, the low pressure structure mainly shows a cross-slot feature (Figs. 11b,c), which is helpful for the transportation of moisture to the rainfall region. The anomalous PV is located not only in the rainfall region but also to the east of the rainfall region. This supported strengthening of the system

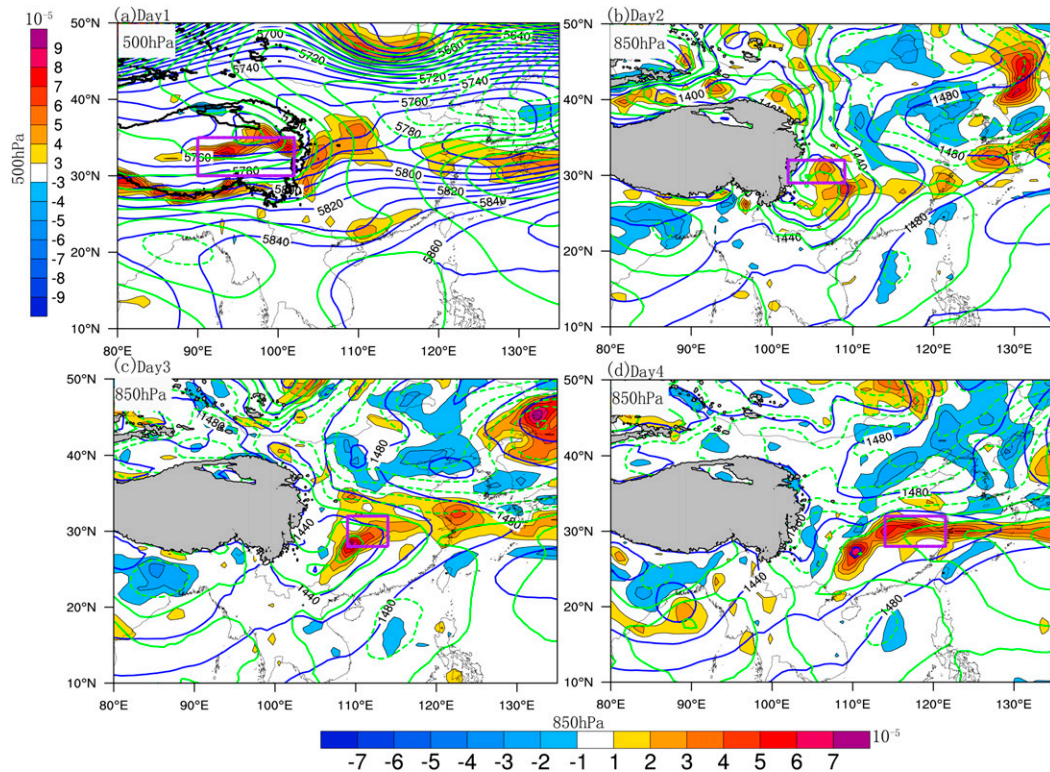


FIG. 11. The inversion results of anomalous geopotential height (green lines; unit: m) at (a) 500 and (b)–(d) 850 hPa from the PV generated by diabatic heating during the heavy rainfall process. The solid green lines represent the positive anomalous values and the dashed green lines represent the negative anomalous values. The blue lines are the geopotential height during the heavy rainfall period. The colored shading is the anomalous PV as shown in Eq. (4). The gray shading is the TP with heights above 3000 m and the purple box is the rainfall as shown in Fig. 4.

and helped it to move toward the east. The positive PV and negative geopotential height were closely coupled with each other. After the rainband moved off the TP, a large PV positive-value region appeared on the east side of the rainfall region, which caused the system to continue to move eastward. There is also a large-PV-value region to the south or southwest of the rainfall region (Figs. 11b–d), which resulted in the moisture being transported aloft and then condensed, giving rise to the diabatic heating. In summary, in the lower layer, the anomalous PV as well as the geopotential height enhanced the development of the low pressure system and made it move eastward. In addition, the diabatic heating is important for the eastward-moving vortex.

e. The moisture conditions for the eastward-moving rainfall process

Hsu et al. (2016) suggested that moisture convergence plays a key role in providing advantageous circumstances for the occurrence of extreme rainfall events. Leung et al. (2018) suggested that both vertical motion and moisture supply are key factors for changing summer rainfall over the middle and lower reaches of the YRB. There are at least three conditions for the occurrence of rainfall. The first is uplift conditions, which can be caused by orographic lift, frontal lift, convergence

lift, and convective lift. The second is atmospheric instability. The third necessary condition is sufficient moisture supply. To look into the details of the third condition, the anomalous water vapor transport flux for the heavy rainfall process was selected (Fig. 12). It is found that during the heavy rainfall, the moisture from the BOB dominated the moisture supply to the rainfall region. When the rainfall moves off the TP, the other moisture channel from the SCS and the western Pacific adds more moisture to the rainfall. Moreover, both channels merge at the southeastern TP. The east of the TP plays a key role in the heavy rainfall in the LRYR, as reported by previous studies (Xu et al. 2008; Li et al. 2016). During the heavy rainfall process, it showed the positive anomaly of sea surface temperature which is favorable for evaporation over the oceans and water vapor transport to the precipitation region. Notably, compared with the climate state, the location of the WPSH is obviously more westward extending during the heavy rainfall process. Although the WPSH is also more westward extending in the initial phase, the rainfall is not yet affected by the WPSH. When the rainband moves off the TP, the WPSH is extended farther west (Figs. 12b–d). The location of the WPSH is helpful for the merging of the moisture at the east of the TP. Moreover, when the rainband move off the TP, the positive anomalous sea surface temperature is extended farther north

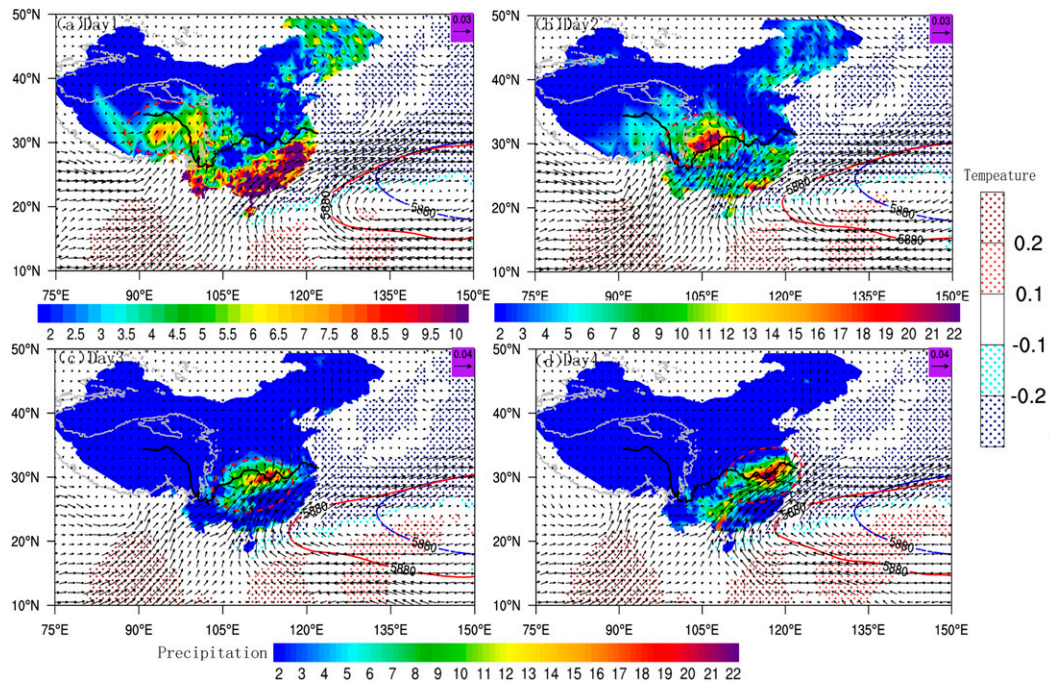


FIG. 12. Column-integrated moisture flux anomaly (vector; unit: $\text{g m}^{-1} \text{s}^{-1}$) on top of rainfall amount (shading; unit: mm day^{-1}) shown in Fig. 4 from days (a) 1, (b) 2, (c) 3, and (d) 4 of the 27 heavy rainfall events. The red line is the geopotential height for extreme state at 500 hPa, and the blue is the geopotential height for climate state. The colored dots represent the anomalous sea surface temperature (unit: K). The black line denotes the Yangtze River and the gray line represents the TP (height at 3000 m).

(Figs. 12b–d), a large amount of water vapor is transported to the rainfall region.

4. Conclusions

The heavy rainfall days over the LYRY that were caused by eastward-moving vortex originated from the TP and moved into the LRYR from 1980 to 2016 were determined and studied. It takes 3–5 days for the vortex structure associated with rainfall to travel from the TP to the LRYR, and most of them took 4 days to travel. Some of the heavy rainfall occurring over the LRYR can be traced back to the vortex structure moving out of the TP. We selected 27 heavy rainfall events over the LYRY that were derived from the TP and traveled for 4 days to reach the LRYR for detailed analysis. These eastward-moving rainfall events represent more than 50% of the total eastward-moving rainfall events.

The differences between the composites of the 27 rainfall cases and the climatology during the study period were used to determine the impacts of both dynamic and thermodynamic processes on the eastward-moving heavy rainfall process.

For the dynamic effect, in the lower level, an anomalous cyclonic structure is found, which is favorable for convergence motion. The moisture from the sea is assembled over the rainfall region and the convergence is helpful for upward motion. At the middle level, the rain region is located in the front of the trough, enhancing the intensity of precipitation. Moreover, the positive absolute vorticity advection in the front

of the trough is helpful for the eastward moving of the low vortex. At higher level, a “dipole” structure was formed. The differences in the wind and geopotential height fields show anomalous low pressure and high pressure structures, similar to trough and ridge structures. The upstream region of the heavy rainfall is located between the low pressure and high pressure systems. The region of rainfall is situated at the fore of the upper trough, which is favorable for developing eastward-moving motion.

In terms of the thermodynamic effect, during the eastward-moving process, the upstream of the rainfall is always influenced by the atmospheric apparent heating. The heating effect enhances the air instability as well as reinforces the convective motion. The warm moist air is pumped from the lower level into the upper level by the processes described previously.

The PV inversion results show that the anomalous PV and negative geopotential height are tightly coupled with each other. In the lower layer, the anomalous geopotential height results in the development and eastward movement of the low pressure system. The PV inversion indicates that the diabatic heating is important for the eastward movement of the vortex.

A comparison between the climatology and the composites of the 27 rainfall events reveals that during the heavy rainfall events, a larger amount of water vapor is transported from the BOB, the SCS, and the western Pacific. The rich moisture supply is a necessary and critical condition for the occurrence of heavy rainfall. Another feature of the heavy rainfall events is

that the WPSH extends farther west, which is also helpful for the merging of moisture at the east of the TP, a key region providing moisture to the rainfall over the LRYR.

In summary, diagnostics of the associated dynamic and thermodynamic processes involved in the heavy rainfall events confirm that the combined action of dynamics and diabatic heating are favorable for the formation, development, and eastward movement of the rainfall.

Acknowledgments. We acknowledge the National Meteorological Information Center of the China Meteorological Administration for providing the observational daily rain dataset (<http://data.cma.cn/>), and the European Centre for Medium-Range Weather Forecasts to support reanalysis data (<http://apps.ecmwf.int/datasets/>). This work was supported by National Research Foundation of Korea (NRF) grant funded by the Korean government (MEST) (Grant 2019R1A6A1A10073437); the Strategic Priority Research Program of Chinese Academy of Sciences (Grant XDA20060401); Swedish STINT, BECC, and MERGE; and National Key Research and Development Project (2018YFC0406602).

REFERENCES

- Black, R. X., and R. Dole, 1993: The dynamics of large-scale cyclogenesis over the North Pacific Ocean. *J. Atmos. Sci.*, **50**, 421–442, [https://doi.org/10.1175/1520-0469\(1993\)050<0421:TDOLSC>2.0.CO;2](https://doi.org/10.1175/1520-0469(1993)050<0421:TDOLSC>2.0.CO;2).
- Chen, Y., and P. M. Zhai, 2016: Mechanisms for concurrent low-latitude circulation anomalies responsible for persistent extreme precipitation in the Yangtze River Valley. *Climate Dyn.*, **47**, 989–1006, <https://doi.org/10.1007/s00382-015-2885-6>.
- Curio, J., R. Schiemann, K. I. Hodges, and A. G. Turner, 2019: Climatology of Tibetan Plateau vortices in reanalysis data and a high-resolution global climate model. *J. Climate*, **32**, 1933–1950, <https://doi.org/10.1175/JCLI-D-18-0021.1>.
- Dee, D. P., and S. Uppala, 2009: Variational bias correction of satellite radiance data in the ERA-Interim reanalysis. *Quart. J. Roy. Meteor. Soc.*, **135**, 1830–1841, <https://doi.org/10.1002/qj.493>.
- , and Coauthors, 2011: The ERA-Interim reanalysis: Configuration and performance of the data assimilation system. *Quart. J. Roy. Meteor. Soc.*, **137**, 553–597, <https://doi.org/10.1002/qj.828>.
- Downton, M. W. and R. A. Pielke, 2005: How accurate are disaster loss data? The case of U.S. flood damage. *Nat. Hazards*, **35**, 211–228, <https://doi.org/10.1007/s11069-004-4808-4>.
- Duan, A. M., and G. X. Wu, 2005: Role of the Tibetan Plateau thermal forcing in the summer climate patterns over subtropical Asia. *Climate Dyn.*, **24**, 793–807, <https://doi.org/10.1007/s00382-004-0488-8>.
- , and Z. X. Xiao, 2015: Does the climate warming hiatus exist over the Tibetan Plateau? *Sci. Rep.*, **5**, 13711, <https://doi.org/10.1038/srep13711>.
- , G. X. Wu, Y. M. Liu, Y. M. Ma, and P. Zhao, 2012: Weather and climate effects of the Tibetan Plateau. *Adv. Atmos. Sci.*, **29**, 978–992, <https://doi.org/10.1007/s00376-012-1220-y>.
- Ge, J., Q. L. You, and Y. Q. Zhang, 2019: Effect of Tibetan Plateau heating on summer heavy extreme precipitation in eastern China. *Atmos. Res.*, **218**, 364–371, <https://doi.org/10.1016/j.atmosres.2018.12.018>.
- Hoskins, B. J., M. E. McIntyre, and A. W. Robertson, 1985: On the use and significance of isentropic potential vorticity maps. *Quart. J. Roy. Meteor. Soc.*, **111**, 877–946, <https://doi.org/10.1002/qj.49711147002>.
- Hsu, H. H., 2003: Relationship between the Tibetan Plateau heating and East Asian summer monsoon rainfall. *Geophys. Res. Lett.*, **30**, 2066, <https://doi.org/10.1029/2003GL017909>.
- Hsu, P. C., J. Y. Lee, and K. J. Ha, 2016: Influence of boreal summer intraseasonal oscillation on rainfall extremes in southern China. *Int. J. Climatol.*, **36**, 1403–1412, <https://doi.org/10.1002/joc.4433>.
- Hu, Y., Y. Deng, Z. M. Zhou, C. G. Cui, and X. Q. Dong, 2018: A statistical and dynamical characterization of large-scale circulation patterns associated with summer extreme precipitation over the middle reaches of Yangtze River. *Climate Dyn.*, **52**, 6213–6228, <https://doi.org/10.1007/s00382-018-4501-z>.
- Huang, Y. Y., and Y. F. Qian, 2004: Relationship between South Asian high and characteristic of precipitation in mid- and lower reaches of Yangtze River and North China (in Chinese). *Plateau Meteor.*, **23**, 68–74, [https://doi.org/1000-0534\(2004\)01-0068-07](https://doi.org/1000-0534(2004)01-0068-07).
- Hunt, K., J. Curio, A. G. Turner, and R. Schiemann, 2018: Subtropical westerly jet influence on occurrence of western disturbances and Tibetan Plateau vortices. *Geophys. Res. Lett.*, **45**, 8629–8636, <https://doi.org/10.1029/2018GL077734>.
- Kukulies, J., D. L. Chen, and M. H. Wang, 2019: Temporal and spatial variations of convection and precipitation over the Tibetan Plateau based on recent satellite observations. Part I: Cloud climatology derived from CloudSat and CALIPSO. *Int. J. Climatol.*, **39**, 5396–5412, <https://doi.org/10.1002/joc.6162>.
- Kundzewicz, Z. W., and Coauthors, 2014: Flood risk and climate change: Global and regional perspectives. *Hydrol. Sci. J.*, **59** (1), 1–28, <https://doi.org/10.1080/02626667.2013.857411>.
- Leung, Y. T., S. Qiu, and W. Zhou, 2018: Modulations of rising motion and moisture on summer precipitation over the middle and lower reaches of the Yangtze River. *Climate Dyn.*, **51**, 4259–4269, <https://doi.org/10.1007/s00382-018-4247-7>.
- Li, C. Q., Q. J. Zuo, X. D. Xu, and S. T. Gao, 2016: Water vapor transport around the Tibetan Plateau and its effect on summer rainfall over the Yangtze River valley. *J. Meteor. Res.*, **30**, 472–482, <https://doi.org/10.1007/s13351-016-5123-1>.
- Li, L., R. H. Zhang, and M. Wen, 2017: Genesis of southwest vortices and its relation to Tibetan Plateau vortices: Genesis of SWVs and its relation to TPVs. *Quart. J. Roy. Meteor. Soc.*, **143**, 2556–2566, <https://doi.org/10.1002/qj.3106>.
- Li, Y., and M. Zhang, 2017: The role of shallow convection over the Tibetan Plateau. *J. Climate*, **30**, 5791–5803, <https://doi.org/10.1175/JCLI-D-16-0599.1>.
- Liu, Y., D. Wang, Z. Liang, and C. Liu, 2016: The structure and development of an extratropical cyclone over northeastern Asia. *SOLA*, **12**, 253–258, <https://doi.org/10.2151/SOLA.2016-050>.
- Lu, Y., and Y. Deng, 2015: Initial transient response of an intensifying baroclinic wave to increase in cloud droplet number concentration. *J. Climate*, **28**, 9669–9677, <https://doi.org/10.1175/JCLI-D-15-0251.1>.
- Qian, Y., M. G. Flanner, L. R. Leung, and W. Wang, 2011: Sensitivity studies on the impacts of Tibetan Plateau snowpack pollution on the Asian hydrological cycle and monsoon climate. *Atmos. Chem. Phys.*, **11**, 1929–1948, <https://doi.org/10.5194/acp-11-1929-2011>.
- Qie, X. S., X. K. Wu, T. Yuan, J. C. Bian, and D. Lu, 2014: Comprehensive pattern of deep convective systems over the Tibetan Plateau–South Asian monsoon region based on TRMM data. *J. Climate*, **27**, 6612–6626, <https://doi.org/10.1175/JCLI-D-14-00076.1>.
- Salinger, M. J., and G. M. Griffiths, 2001: Trends in New Zealand daily temperature and rainfall extremes. *Int. J. Climatol.*, **21**, 1437–1452, <https://doi.org/10.1002/joc.694>.
- Shi, X. Y., Y. Q. Wang, and X. D. Xu, 2008: Effect of mesoscale topography over the Tibetan Plateau on summer precipitation in China: A regional model study. *Geophys. Res. Lett.*, **35**, L19707, <https://doi.org/10.1029/2008GL034740>.

- Teubler, F., and M. Riemer, 2016: Dynamics of Rossby wave packets in a quantitative potential vorticity–potential temperature framework. *J. Atmos. Sci.*, **73**, 1063–1081, <https://doi.org/10.1175/JAS-D-15-0162.1>.
- Wang, F., and S. Yang, 2017: Regional characteristics of long-term changes in total and extreme precipitation over China and their links to atmospheric–oceanic features. *Int. J. Climatol.*, **37**, 751–769, <https://doi.org/10.1002/joc.4737>.
- Wang, G. Z., X. Li, X. H. Wu, and J. Yu, 2015: The rainstorm comprehensive economic loss assessment based on CGE model: Using a July heavy rainstorm in Beijing as an example. *Nat. Hazards*, **76**, 839–854, <https://doi.org/10.1007/s11069-014-1521-9>.
- Wang, M. R., J. Wang, A. M. Duan, and Y. M. Liu, 2019: Quasi-bi-weekly impact of the atmospheric heat source over the Tibetan Plateau on summer rainfall in eastern China. *Climate Dyn.*, **53**, 4489–4504, <https://doi.org/10.1007/s00382-019-04798-x>.
- Winters, A. C., and J. E. Martin, 2017: Diagnosis of a North American polar–subtropical jet superposition employing piecewise potential vorticity inversion. *Mon. Wea. Rev.*, **145**, 1853–1873, <https://doi.org/10.1175/MWR-D-16-0262.1>.
- Wu, Z., J. Li, J. He, and Z. Jiang, 2006: Occurrence of droughts and floods during the normal summer monsoons in the mid- and lower reaches of the Yangtze River. *Geophys. Res. Lett.*, **33**, L05813, <https://doi.org/10.1029/2005GL024487>.
- Xiao, M. Z., Q. Zhang, and V. P. Singh, 2014: Influences of ENSO, NAO, IOD, and PDO on seasonal precipitation regimes in the Yangtze River basin, China. *Int. J. Climatol.*, **35**, 3556–3567, <https://doi.org/10.1002/joc.4228>.
- Xu, X. D., C. G. Lu, X. H. Shi, and S. T. Gao, 2008: World water tower: An atmospheric perspective. *Geophys. Res. Lett.*, **35**, L20815, <https://doi.org/10.1029/2008GL035867>.
- , —, Y. H. Ding, X. H. Shi, Y. D. Guo, and W. H. Zhu, 2013: What is the relationship between China summer precipitation and the change of apparent heat source over the Tibetan Plateau? *Atmos. Sci. Lett.*, **14**, 227–234, <https://doi.org/10.1002/asl2.444>.
- , and Coauthors, 2017: Are precipitation anomalies associated with aerosol variations over eastern China? *Atmos. Chem. Phys.*, **17**, 8011–8019, <https://doi.org/10.5194/acp-17-8011-2017>.
- Yang, K., H. Wu, J. Qin, C. G. Lin, W. J. Tang, and Y. Y. Chen, 2014: Recent climate changes over the Tibetan Plateau and their impacts on energy and water cycle: A review. *Global Planet. Change*, **112**, 79–91, <https://doi.org/10.1016/j.gloplacha.2013.12.001>.
- Zhang, L., and T. Zhou, 2015: Drought over East Asia: A review. *J. Climate*, **28**, 3375–3399, <https://doi.org/10.1175/JCLI-D-14-00259.1>.
- Zhang, Q., G. X. Wu, and Y. F. Qian, 2002: The bimodality of the 100 hPa South Asia high and its relationship to the climate anomaly over East Asia in summer. *J. Meteor. Soc. Japan*, **80**, 733–744, <https://doi.org/10.2151/jmsj.80.733>.
- , C. Y. Xu, Z. Zhang, Y. D. Chen, C. L. Liu, and H. Lin, 2008: Spatial and temporal variability of precipitation maxima during 1960–2005 in the Yangtze River basin and possible association with large-scale circulation. *J. Hydrol.*, **353**, 215–227, <https://doi.org/10.1016/j.jhydrol.2007.11.023>.
- Zhang, S. L., and S. Y. Tao, 2002: The influences of Tibetan Plateau of weather anomalies over Chang Jiang River in 1998. *J. Meteor. Res.*, **60**, 442–452.
- Zhao, P., and L. X. Chen, 2001: Interannual variability of atmospheric heat source/sink over the Qinghai-Xizang (Tibetan) Plateau and its relation to circulation. *Adv. Atmos. Sci.*, **18** (1), 106–116, <https://doi.org/10.1007/s00376-001-0007-3>.
- Zhao, Y., X. D. Xu, B. Chen, and Y. J. Wang, 2016a: The upstream “strong signals” of the water vapor transport over the Tibetan Plateau during a heavy rainfall event in the Yangtze River Basin. *Adv. Atmos. Sci.*, **33**, 1343–1350, <https://doi.org/10.1007/s00376-016-6118-7>.
- , —, T. L. Zhao, H. X. Xu, F. Mao, H. Sun, and Y. H. Wang, 2016b: Extreme precipitation events in East China and associated moisture transport pathways. *China Earth Sci.*, **59**, 1854–1872, <https://doi.org/10.1007/s11430-016-5315-7>.
- , —, Z. Ruan, B. Chen, and F. Wang, 2018: Precursory strong-signal characteristics of the convective clouds of the central Tibetan Plateau detected by radar echoes with respect to the evolutionary processes of an eastward-moving heavy rainstorm belt in the Yangtze River Basin. *Meteor. Atmos. Phys.*, **131**, 697–712, <https://doi.org/10.1007/s00703-018-0597-2>.
- , —, L. P. Liu, R. Zhang, H. X. Xu, Y. J. Wang, and J. Li, 2019a: Effects of convection over the Tibetan Plateau on rainstorm in the downstream area of the Yangtze River Basin. *Atmos. Res.*, **219**, 24–35, <https://doi.org/10.1016/j.atmosres.2018.12.019>.
- , and Coauthors, 2019b: The large-scale circulation patterns responsible for heavy precipitation over the North China Plain in midsummer. *J. Geophys. Res. Atmos.*, **124**, 12 794–12 809, <https://doi.org/10.1029/2019JD030583>.
- Zhong, L., Z. Zhang, L. Chen, J. H. Yang, and F. L. Zou, 2016: Application of the Doppler weather radar in real-time quality control of hourly gauge precipitation in eastern China. *Atmospheric*, **172–173**, 109–118, <https://doi.org/10.1016/j.atmosres.2015.12.016>.
- Zong, Y., and X. Chen, 2000: The 1998 flood on the Yangtze, China. *Nat. Hazards*, **22**, 165–184, <https://doi.org/10.1023/A:1008119805106>.